

PACS 78.20.-e, 82.80.Jk

Optical and morphological properties of tetragonal $\text{Cu}_2\text{ZnSnS}_4$ thin films grown from sulphide precursors at lower temperatures

I.S. Babichuk^{1,*}, V.O. Yukhymchuk¹, M.O. Semenenko¹, N.I. Klyui¹, R. Caballero², O.M. Hreshchuk¹, I.S. Lemishko³, I.V. Babichuk⁴, V.O. Ganus¹, and M. Leon²

¹*V. Lashkaryov Institute of Semiconductor Physics, NAS of Ukraine, 45, prospect Nauky, 03028 Kyiv, Ukraine;*

²*Universidad Autónoma de Madrid, Departamento de Física Aplicada, C/Francisco Tomás y Valiente 7, E-28049 Madrid, Spain;*

³*National Technical University of Ukraine "Kyiv Polytechnic Institute", 37, prospect Peremohy, 03056 Kyiv, Ukraine;*

⁴*V. Vernadsky Institute of General and Inorganic Chemistry, NAS of Ukraine, 32/34, prospect Akademika Palladina, 03142 Kyiv, Ukraine*

**Corresponding author. Phone: 38(044) 525-83-03; e-mail: babichuk@isp.kiev.ua*

Abstract. Optical constants of $\text{Cu}_2\text{ZnSnS}_4$ thin films formed using thermal annealing of pre-deposited layers of copper, zinc and tin sulphides on glass substrates at different temperatures and ambient atmosphere were determined. It has been shown that films grown at lower temperatures have the tetragonal structure of kesterite, and the corresponding value of the optical band gap is 1.47 eV.

Keywords: Raman spectroscopy, SEM, optical constants, kesterite, CZTS.

Manuscript received 25.02.14; revised version received 30.07.14; accepted for publication 16.09.14; published online 30.09.14.

1. Introduction

Nowadays photovoltaic devices around the world provide production of about 20 GW of electrical power. Almost 90% of them are based on silicon solar cells, the effectiveness of which reaches theoretical limits, and their cost is still quite high. One of the solutions to reduce the cost of manufacturing photovoltaic modules is use of thin-film technology. However, in this respect, single-crystal silicon is not an effective material, because it has an indirect energy band structure and, consequently, it has a relatively low value of absorption of solar radiation in the visible and near infrared bands (1-2 eV). Switching to involving the direct energy band materials can significantly reduce the thickness of semiconductor layer that efficiently absorbs incident radiation in this range.

High interest in investigation of quaternary semiconductor compounds based on chalcogenides and widespread elements of groups II and IV, for example of the $\text{Cu}_2\text{B}^{\text{II}}\text{C}^{\text{IV}}\text{S}_4$ type, a typical representative of which is $\text{Cu}_2\text{ZnSnS}_4$ (CZTS), is caused by search of new materials for designing solar cells. Their direct energy band determining the high interband absorption coefficient for solar radiation in the visible spectral range is turn-point to make solar cells to be cheaper. The other two important factors for potential use of CZTS in solar cell application are widespread in the crust of the constituent elements and their sustainability in manufacturing processes and application.

Up to date, the efficiency of CZTS-based solar cells has reached the level close to 12.6% [1]. To increase the efficiency, several problems should be solved. They are collected in series as follows: the

presence of non-stoichiometry elemental composition of CZTS and the concentration of intrinsic defects in the crystallographic structure and conformably in the energy band gap; properties of CZTS by coexistence of crystallographic phases and by the possible impurities of secondary binary and ternary compounds formed during the synthesis.

In this work, optical and vibrational properties of $\text{Cu}_2\text{ZnSnS}_4$ thin films obtained by thermal annealing the pre-deposited binary compounds ZnS, CuS and SnS on glass substrates were investigated. Annealing was carried out at two different temperatures and in two different gas atmospheres. To determine optical constants of this material, the spectra of light reflection were analyzed at normal incidence, which is convenient from the viewpoint of conversion of complex-conjugate functions using dispersion Kramers-Kronig integrals [2]. It is known that, to obtain reliable results, if using the dispersion Kramers-Kronig integrals, precise measurements of reflection spectra in the whole optical range should be carried out. In addition, their use for calculating the optical constants suggests that the experimental studies are performed with fairly thick material, for which the reflection spectrum is recorded between two semi-infinite media.

2. Experimental technique

In this work, $\text{Cu}_2\text{ZnSnS}_4$ thin films were obtained using deposition of binary compounds ZnS, CuS and SnS on glass substrates with pre-deposited molybdenum as a bottom layer. Annealing was carried out at two different temperatures 370 and 390 °C in air and in nitrogen atmosphere. The use of relatively low temperature was applied to compare with results of deposition of similar structures on flexible organic polymer films.

Reflection spectra were recorded using the spectrometer Shimadzu UV-3600, and surface morphology was investigated applying the scanning electron microscope (SEM) Tescan Mira 3 LMU. Component compositions were determined using energy-dispersive X-ray spectroscopy (EDX) with Oxford instruments INCA x-sight that was built in the SEM. To investigate structural properties of $\text{Cu}_2\text{ZnSnS}_4$, the method of m-Raman spectroscopy (T64000 Horiba Jobin Yvon) was employed. For excitation of Raman spectra, radiation of Ar^+ -laser with the wavelength 514.5 nm was used. The power of laser radiation was chosen sufficiently minimal (the laser power density was $0.1 \text{ mW}/\mu\text{m}^2$) in order not to add changes in the film structure during these measurements. All the measurements were performed at room temperature. Moreover, Raman spectra were recorded in different parts of each sample, because of morphology and the phase inhomogeneities on the top of film surface were visible in the optical microscope. After that, the collected results were averaged to obtain the average parameters of the existing medium as well as to establish the nature of some crystalline phases that segregated.

Spectra of photoluminescence (PL) were recorded at the temperature of liquid nitrogen. The excitations of spectra were carried out upon the incidence of light of Nd: YAG laser with the wavelength 532 nm.

3. Results and discussion

It is known that, during high-temperature annealing, atoms of sulphur rapidly evaporate from the surface of CZTS [3]. Being based on this fact, to obtain compounds with stoichiometric component ratio (2:1:1:4) annealing should be carried out in atmosphere of sulphur. Moreover, in the course of annealing in sulphur atmosphere, zinc first takes all of the sulphur saturation according to the electrochemical activity of a number of metals. To clarify this mismatch, it should be first analyzed the reactions of formation of sulphides by using standard oxidation-reduction potentials for binary compounds that were collected in the table [4].

We can see from Table 1 that the first metal will be reduced to atomic state in the process is copper. Therefore, observation of the CuS and Cu_2S phases in the synthesized film after sulphurization is the most probable. Indeed, this assumption is confirmed by the results of the studies of such structures by Raman spectroscopy and X-ray diffraction (XRD) in many works [3, 5-7]. On the other hand, the CuS and Cu_2S phases are less stable in contrast to ZnS and MoS_2 . As can be seen from the Table 2, the standard molar enthalpy of their formation is minimal in its absolute value for a number of binary compounds [4, 8].

The standard molar enthalpy of formation of any substance is a measure of its stability. The higher is the absolute value of the enthalpy for formation of such compounds, as we assume, the more stable is this compound. Therefore, during their synthesizing CZTS films were formed using such compounds as ZnS, MoS_2 , CuS, Cu_2S .

Table 1. Oxidation-reduction reactions.

Electrode processes	$E, \text{ V}$
$\text{CuS} + 2\text{e}^- = \text{Cu} + \text{S}^{2-}$	-0.76
$\text{SnS} + 2\text{e}^- = \text{Sn} + \text{S}^{2-}$	-0.87
$\text{Cu}_2\text{S} + 2\text{e}^- = 2\text{Cu} + \text{S}^{2-}$	-0.89
$\text{ZnS} + 2\text{e}^- = \text{Zn} + \text{S}^{2-}$	-1.405

Table 2. Standard molar enthalpy values.

Sulfides	$\Delta H^\circ, \text{ kJ/mol}$
CuS	-53.1
Cu_2S	-53.1
SnS_2	-82.4
SnS	-110.2
ZnS	-205.4
MoS_2	-248.1

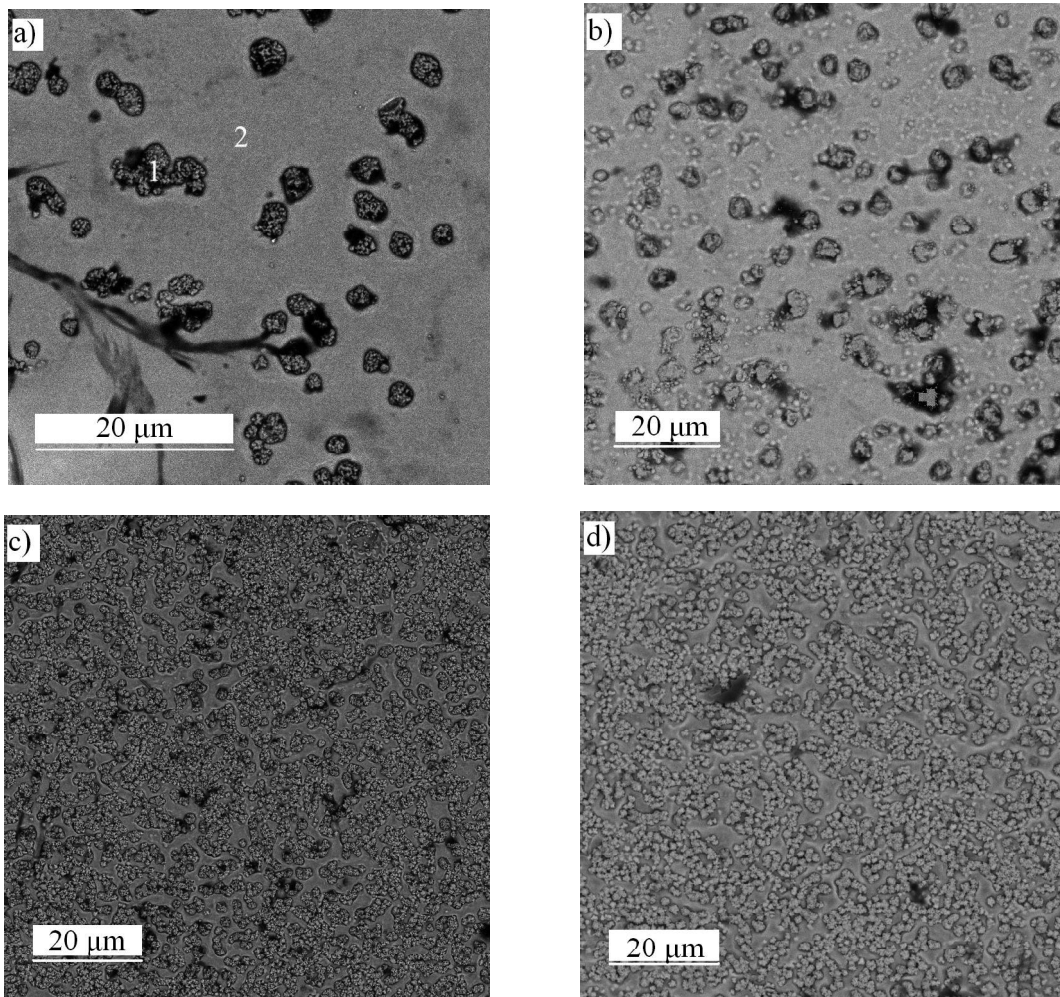


Fig. 1. SEM images of the surface of CZTS films grown at 370° C (a, b) and 390° C (c, d) in N₂ (a, c) and air (b, d).

As can be seen from Fig. 1, surface morphology of CZTS films strongly depends on technological conditions during their synthesis: annealing temperature and atmosphere of processing. The increase in the temperature of synthesis only by 20 °C from 370 to 390 °C results in significant changes in surface morphology of the formed CZTS films. To determine the component structure of formed films and individual phase inclusions, local-EDRS studies were carried out in various regions of the film surface. For separating the bands in the EDRS spectrum obtained from the individual elements, the energy of electrons used for sensing was relatively large, resulting in a contribution to the range of items from all over the film thickness. However, in this case, it is possible to get information about the elemental composition inhomogeneities arising on the surface of the films during its synthesis (Fig. 1). From these investigations, it was found that the elemental composition of morphological heterogeneity (Fig. 1a, region 1) corresponds to the composition enriched with Cu (Cu-rich). At the same time, in areas where the film is homogeneous (Fig. 1a, region 2) the

ratio of the components Cu:Zn:Sn:S is closer to the stoichiometric one, although here we observed a little bit overstated content of Cu and depletion of Sn.

The Raman spectra of the CZTS films and their corresponding deconvoluted components (Lorentzians) are presented in Fig. 2. The films were formed at the temperature close to 390 °C in air (a) and nitrogen (b) atmospheres. As it is seen from the spectra shown in Figs. 2a and 2b, the main bands of the Raman spectra of CZTS films formed in air and nitrogen (N₂) at the temperature 370 °C were practically indistinguishable. But in the addition to the main A-symmetry band of CZTS, a very intense band at the frequency 473 cm⁻¹ is presented in the spectrum of the film formed in nitrogen at 370 °C (Fig. 2c, inset), which corresponds to the vibrations of Cu₂S compound [9, 10]. The main contribution to the obtained spectra is given by A-symmetry bands of CZTS compound with the frequencies 288 and 337(336)cm⁻¹ and bands with the frequencies 254(251), 312(308), 358(360), 372 cm⁻¹, corresponding to the vibrations of E- and B-symmetry

and discussed in detail in [10-15]. The bands with the frequencies $\sim 412(410)$ cm^{-1} correspond to the vibrations of the MoS_2 compound [16]. Raman spectra of the films that were synthesized in air (Fig. 2a) are slightly different from the spectra of the films formed in nitrogen (Fig. 2b). Although, it should be noted that the frequency position of Raman bands in respect with the films formed in nitrogen atmosphere is somewhat lower. During annealing, the presence of oxygen in air can cause interaction of individual elements in CZTS films with oxygen, which is reflected in a decrease of the vibrational frequency of the main modes inherent to material. Analysis of half-widths of Raman bands in the films formed in different atmospheres showed that their values for the bands in the first case are less than that of the latter one by 4 cm^{-1} . Perhaps, it is caused by partial oxidation of the binary and ternary phases formed in the course of the synthesis of CZTS. It results in reduction of their contribution to the mechanical stress stability of main material and, therefore, reduction of the half-width of the bands occurs. The half-widths of the bands observed in the abovementioned films are larger by ~ 8 cm^{-1} as compared with the similar films obtained at higher temperatures of synthesis (475...600 $^{\circ}\text{C}$) (see Ref. [13]). The obtained results should be improved to reach values [13], however, the use of lower temperatures of annealing is a prerequisite to pronounce the perspectives of formation of the structures on the flexible organic polymer films that are not suitable to be treated at higher temperatures.

Thus, to make the analysis of the Raman spectra of all the films, we conclude that the annealing temperature within the range from 370 to 390 $^{\circ}\text{C}$ does not provide a significant effect on the frequency position and intensity of bands. But, when the sample is formed at one temperature, but in different atmospheres, the corresponding spectra differ quite significantly from each other (Fig. 2).

Optical reflection spectra $R(\lambda)$ of the CZTS film that were obtained under different technological conditions are shown in Fig. 3. Analysis of the experimental data showed that the reflections of the films with increase of the annealing temperature are significantly reduced, namely, in air by 8% and in N_2 – 25%. A significant decrease in the reflectivity of the films annealed in N_2 can be attributed to the microstructure of the film. SEM images (Figs. 1a and 1b) show that the films annealed at 370 $^{\circ}\text{C}$ have a relatively lower surface density of microcrystalline grains as compared with that on the film surface (Figs. 1c and 1d), when being annealed at 390 $^{\circ}\text{C}$. The increase in the annealing temperature by 20 $^{\circ}\text{C}$ results in a significant decrease of the optical reflectivity. This result is important for designing the photoelectric multiplier, because the low reflection coefficient of the film allows to absorb more solar energy and, consequently, to increase efficiency.

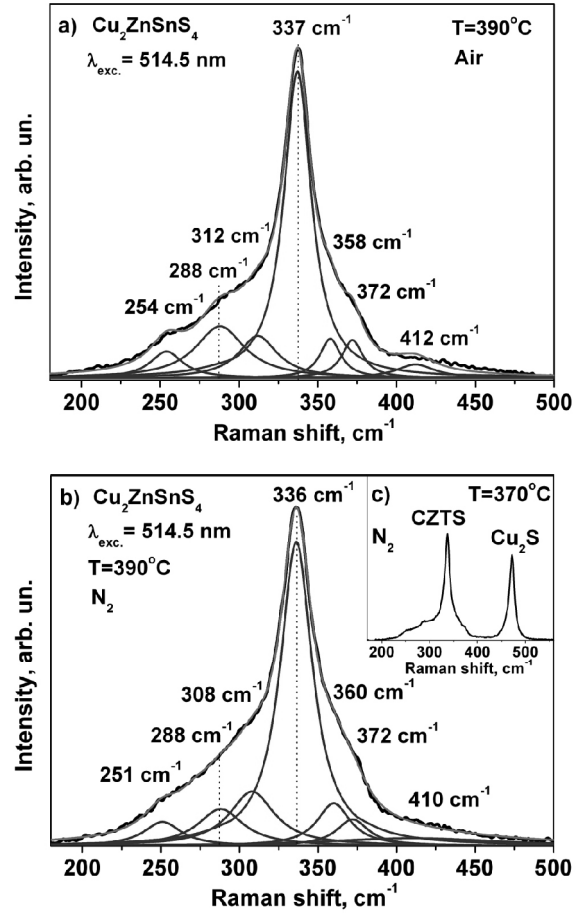


Fig. 2. Raman spectra of CZTS films grown at 390 $^{\circ}\text{C}$ in air (a) and N_2 (b) with deconvoluted components (c); 370 $^{\circ}\text{C}$ in N_2 .

Optical constants of CZTS films were determined using reflection spectra within the range from 380 to 1600 nm. As well known, it is possible to determine the complex index of refraction using the Fresnel equations for the reflection function at the normal incidence of the light beam on the film, according to the formula:

$$R(\omega) = |R'(\omega)|^{1/2} e^{i\theta(\omega)} = \left(\frac{\tilde{n}(\omega) - 1}{\tilde{n}(\omega) + 1} \right), \quad (1)$$

where, $\tilde{n}(\omega) = n(\omega) \pm ik(\omega)$ is the complex index of refraction; n , k are real and imaginary components.

The function of the reflection is related to the Fourier transformation as follows:

$\ln R(\omega) = \frac{1}{2} \ln |R'(\omega)| \pm i\theta(\omega)$. In this case, the phase shift between the incident and reflected rays θ can be determined from the Kramers–Kronig dispersion integral [17]:

$$\theta(\omega_0) = \frac{\omega_0}{\pi} \int_0^{\infty} \frac{\ln |R'(\omega)| - \ln |R'(\omega_0)|}{\omega^2 - \omega_0^2} d\omega, \quad (2)$$

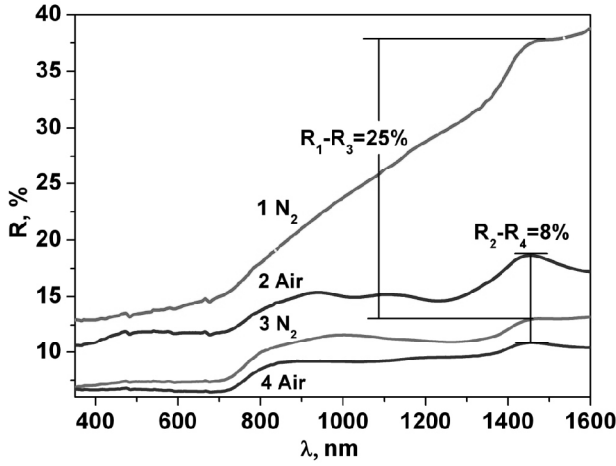


Fig. 3. Reflectance spectra of CZTS films grown at 370 °C (1, 2) and 390 °C (3, 4).

After numerical integration of the dispersion integrals by using the trapezoidal rule with the step 1 meV, the complex refractive index and its components can be determined from the following formula:

$$\tilde{n}(\omega) = \frac{n_L + |R'(\omega)|^{1/2} e^{i\theta(\omega)}}{n_L - |R'(\omega)|^{1/2} e^{i\theta(\omega)}} \quad (3)$$

where, n_L is the refractive index of air.

It is known that the complex dielectric function and the absolute value of the refractive index are linked by equations below:

$$\varepsilon(\omega) = \tilde{n}^2 = \varepsilon_1(\omega) \pm i\varepsilon_2(\omega),$$

$$\varepsilon_1(\omega) = n(\omega)^2 - k(\omega)^2,$$

$$\varepsilon_2(\omega) = 2n(\omega)k(\omega),$$

$$n(\omega) = \sqrt{\frac{\sqrt{\varepsilon_1(\omega)^2 + \varepsilon_2(\omega)^2} + \varepsilon_1(\omega)}{2}}, \quad (4)$$

$$k(\omega) = \sqrt{\frac{\sqrt{\varepsilon_1(\omega)^2 + \varepsilon_2(\omega)^2} - \varepsilon_1(\omega)}{2}}.$$

Calculation of spectral dependences for optical constants of CZTS films: the refractive $n(h\nu)$ and extinction $k(h\nu)$ indexes, the real $\varepsilon_1(h\nu)$ and imaginary $\varepsilon_2(h\nu)$ parts of the complex dielectric function ε was performed using packages of the applied MathCad software. The spectral dependences of $n(h\nu)$ and $k(h\nu)$ are shown in Fig. 4. They were calculated from the latter two ones by using the equation (4). Fig. 4 shows that the optical constants $n(h\nu)$ and $k(h\nu)$ decrease with increasing the photon energy $h\nu$. Variation of the real $\varepsilon_1(h\nu)$ and imaginary $\varepsilon_2(h\nu)$ parts of the dielectric function is similar to that observed for the optical constants $n(h\nu)$ and $k(h\nu)$.

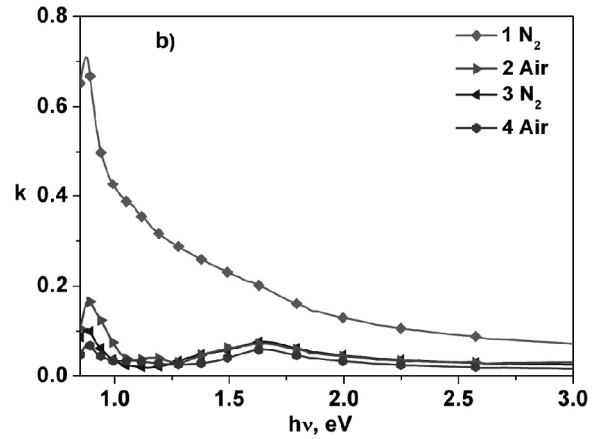
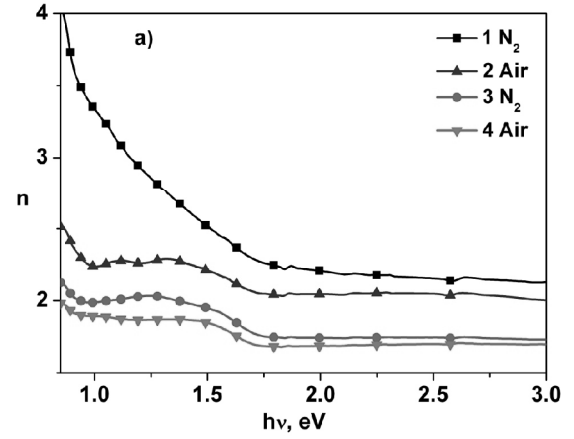


Fig. 4. Spectra of optical functions: a) refractive index $n(h\nu)$; b) extinction coefficient $k(h\nu)$ of CZTS films obtained at 370 °C (1, 2) and 390 °C (3, 4).

In Fig. 5a the spectra of the absorption coefficient $\alpha(h\nu)$ of the films versus photon energy are presented according to the treatments. These spectra were transferred from the reflection spectra by using the dispersion integrals. It should be noted that it does not lead to the significant errors in calculations, from the condition that the film thickness CZTS was grown thicker than 1 μm . It is caused by the high absorption of light by thicker films and decrease of light interference inside the glass-CZTS interface. As shown in Fig. 5a, the increase in absorption coefficient in the low energy region ($h\nu < 1$ eV) is quite sharp. An increase of the slope of the absorption curve is observed near the absorption edge for the CZTS film except the film annealed in nitrogen at 370 °C, for which the absorption coefficient declines of linearity in this region. The same situation is observed for the other films in the range ($h\nu > 1.7$ eV).

In Fig. 5b the calculated absorption spectra are plotted in the Tauc coordinates for direct allowed optical transitions, which makes it possible to estimate effects of the atmosphere presences and the temperature of the annealing on the value of optical energy gap. These

values are slightly less as compared with the data typical for films with a tetragonal like kesterite structure for which the optical band gap $E_g = 1.5$ eV (see Ref. [18]). This mismatch may appear due to availability of structural defects composed in the films both on the surface and in the bulk. In this issue, the inclusion with the energy lower than the value of E_g can affect on the optical energy gap. But among them, we can see that even at low annealing temperatures (390 °C) in both kinds of atmospheres, in which the films were formed, values of E_g are very close to that discussed by the authors in Refs. [18-20]. Moreover, PL spectra of CZTS films were investigated at the temperatures near 80 K. They had somewhat asymmetric broad band with the peak at 1.26 eV. There are several explanations for these features. One of them, as we assume and suggested in [21, 22] for structures similar to CZTS at a low concentration of doping elements, the dominant radiation was caused by recombination of donor-acceptor pairs or transition of electrons from the conduction band to the acceptor level [23].

4. Conclusion

Analysis of the Raman spectra of the films $\text{Cu}_2\text{ZnSnS}_4$ that were formed by thermal annealing previously deposited of precursors layers based on copper, zinc and tin sulphides on glass substrates at different temperatures and in different surrounding atmospheres showed that they have a tetragonal structure of kesterite. Thus, it has been shown that the use of sulphides of copper, tin and zinc, in contrast to corresponding pure metals during the synthesis of these compounds, eliminates the need for the additional annealing in the atmosphere of sulfur to achieve stoichiometric structure. It is shown that changes of the temperature of the annealing from 370 to 390 °C have no significant effect on the features of the Raman spectra. At the same time, changes in the atmosphere in the course of the treatments result in the shift of the frequency of the bands and change in their intensities.

From the reflectance spectra, the optical constants of the formed films were calculated. It has been shown that increase of the synthesis temperature by only 20 °C from 370 to 390 °C leads to a significant increase of the surface density of microcrystalline grains. It reduces the reflection coefficient of the film and provides more efficient light absorption. Therefore, conversion of light to electricity would be more efficient. From our calculations of the absorption spectra, the average estimated energy band gap of films was approximately 1.47 eV.

This research is supported by the People Programme (Marie Curie Actions) of the European Union's Seventh Framework Program FP7 under REA grant agreement 269167 (PVICOKEST) and grant OPTEC as well as State Fund for Fundamental Research of Ukraine (bilateral Belarussian-Ukrainian project no. 54.1/005).

References

1. W. Wang, M.T. Winkler, O. Gunawan, T. Gokmen, T.K. Todorov, Y. Zhu, D.B. Mitzi, Device characteristics of CZTSSe thin-film solar cells with 12.6% efficiency // *Adv. Energy Materials*, **4**(7), p. 1-5 (2014).
2. P. Bruzzoni, R.M. Carranza, J.R. Collet Lacoste, E.A. Crespo, Kramers-Kronig transforms calculation with a fast convolution algorithm // *Electrochimica Acta*, **48**, p. 341-347 (2002).
3. M. Espindola-Rodriguez, M. Placidi, O. Vigil-Galán, V. Izquierdo-Roca, X. Fontané, A. Fairbrother, D. Sylla, E. Saucedo, A. Pérez-Rodríguez, Compositional optimization of photovoltaic grade $\text{Cu}_2\text{ZnSnS}_4$ films grown by pneumatic spray pyrolysis // *Thin Solid Films*, **535**, p. 67-72 (2013).
4. V.A. Rabinovich, Z.Ya. Havich, *Concise Chemical Directory*. Chemistry, Leningrad, 1991.

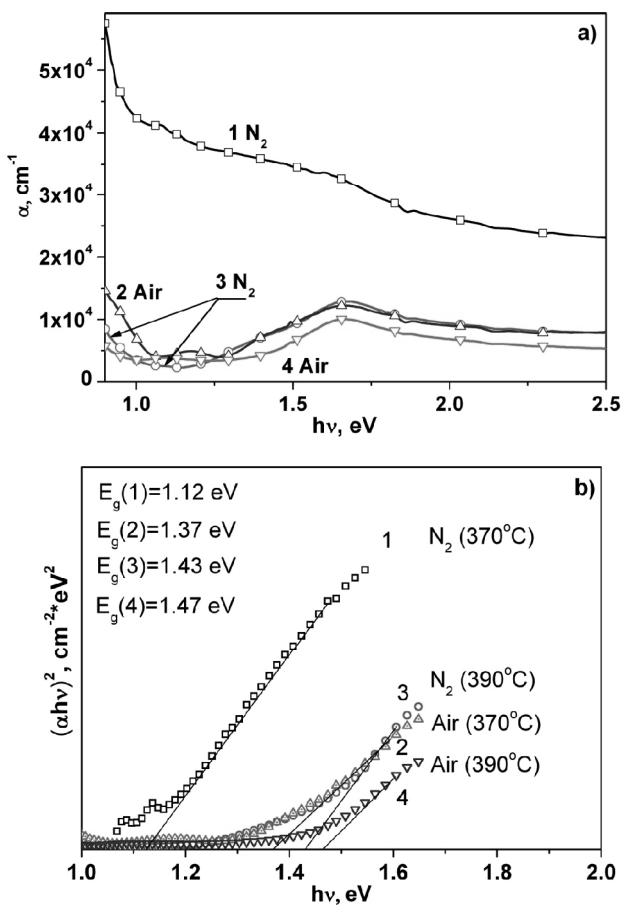


Fig. 5. Spectra of the absorption coefficient of CZTS films: a) grown at 370 °C (1, 2) in N_2 and at 390 °C (3, 4) in air; b) in the Tauc coordinates for the case of direct allowed optical transitions.

5. S. Schorr, The crystal structure of kesterite type compounds: a neutron and x-ray diffraction study // *Solar Energy Materials and Solar Cells*, **95**, p. 1482-1488 (2011).
6. I.D. Olekseyuk, E.V. Dudchak, L.V. Piskach, Phase equilibria in the $\text{Cu}_2\text{S-ZnS-SnS}_2$ system // *J. Alloys and Compounds*, **368**, p. 135-143 (2004).
7. A. Fairbrother, X. Fontané, V. Izquierdo-Roca, M. Espindola-Rodriguez, S. Lopez-Marino, M. Placidi, L. Calvo-Barrio, A. Perez-Rodriguez, E. Saucedo, On the formation mechanisms of Zn-rich $\text{Cu}_2\text{ZnSnS}_4$ films prepared by sulfurization of metallic stacks // *Solar Energy Materials & Solar Cells*, **112**, p. 97-105 (2013).
8. A.J. Jackson, A. Walsh, Ab initio thermodynamic model of $\text{Cu}_2\text{ZnSnS}_4$ // *J. Mater. Chem. A*, **2**, p. 7829-7836 (2014).
9. P.A. Fernandes, P.M.P. Salome, A.F. da Cunha, Growth and Raman scattering characterization of $\text{Cu}_2\text{ZnSnS}_4$ thin films // *Thin Solid Films*, **517**, p. 2519-2523 (2009).
10. I.S. Babichuk, V.O. Yukhymchuk, V.M. Dzhagan, M.Ya. Valakh, M. Leon, I.B. Yanchuk, E.G. Gule, O.M. Greshchuk, Thin films of $\text{Cu}_2\text{ZnSnS}_4$ for solar cells: optical and structural properties // *Functional Materials*, **20**(2), p. 186-191 (2013).
11. X. Fontane, V. Izquierdo-Rosa, E. Saucedo, S. Schorr, V.O. Yukhymchuk, M.Ya. Valakh, A. Perez-Rodriguez, J.R. Morante, Vibrational properties of stannite and kesterite type compounds: Raman scattering analysis of $\text{Cu}_2(\text{Fe,Zn})\text{SnS}_4$ // *J. Alloys and Compounds*, p. 190-194 (2012).
12. A. Khare, B. Himmetoglu, M. Johnson, D.J. Norris, M. Cococcioni, E.S. Aydil, Calculation of the lattice dynamics and Raman spectra of copper zinc tin chalcogenides and comparison to experiments // *J. Appl. Phys.* **111**(8), 083707-083716 (2012).
13. R. Caballero, E. Garcia-Llamas, J.M. Merino, M. León, I. Babichuk, V. Dzhagan, V. Strelchuk, M. Valakh, Non-stoichiometry effect and disorder in $\text{Cu}_2\text{ZnSnS}_4$ thin films obtained by flash evaporation: Raman scattering investigation // *Acta Materialia*, **65** p. 412-417 (2014).
14. M.Ya. Valakh, O.F. Kolomys, S.S. Ponomaryov, V.O. Yukhymchuk, I.S. Babichuk, V. Izquierdo-Rosa, E. Saucedo, A. Perez-Rodriguez, J.R. Morante, S. Schorr, I.V. Bodnar, Raman scattering and disordering effect in $\text{Cu}_2\text{ZnSnS}_4$ // *Phys. Status Solidi (RRL) – Rapid Research Letters*, **7**(4), p. 258-261 (2013).
15. P. Schütz, A.K. Alves, C.P. Bergmann, Effect of the in-air heat treatment in the phase formation and morphology of electrospun $\text{Cu}_2\text{ZnSnS}_4$ fibers // *Ceramics Intern.* **40**(8), p. 11551-11557 (2014).
16. S. Chen, X.G. Gong, Electronic structure and stability of quaternary chalcogenide semiconductors derived from cation cross-substitution of II-VI and I-III-VI₂ compounds // *Phys. Rev. B*, **79**, p. 165211-165221 (2009).
17. M. Cardona, D.L. Greenaway, Optical properties and band structure of group IV-VI and group V materials // *Phys. Rev.* **133**(6A), p. A1685-A1697 (1964).
18. M. Ikhlusal Amal, Kyoo Ho Kim, Structural and optical properties of sulfurized $\text{Cu}_2\text{ZnSnS}_4$ thin films from Cu-Zn-Sn alloy precursors // *J. Mater. Sci.: Materials in Electronics*, **24**(2), p. 559-566 (2013).
19. R.B.V. Chalapathy, G.S. Jung, B.T. Ahn, Fabrication of $\text{Cu}_2\text{ZnSnS}_4$ films by sulfurization of Cu/ZnSn/Cu precursor layers in sulfur atmosphere for solar cells // *Solar Energy Materials and Solar Cells*, **95**(12), p. 3216-3221 (2011).
20. P.K. Sarswat, M.L. Free, A study of energy band gap versus temperature for $\text{Cu}_2\text{ZnSnS}_4$ thin films // *Phys. B: Condens. Matter*, **407**(1), p. 108-111 (2012).
21. J.P. Leitao, N.M. Santos, P.A. Fernandes, P.M.P. Salome, A.F. da Cunha, J.C. Gonzalez, G.M. Ribeiro, F.M. Matinaga, Photoluminescence and electrical study of fluctuating potentials in $\text{Cu}_2\text{ZnSnS}_4$ -based thin films // *Phys. Rev. B*, **84**, 024120–024128 (2011).
22. A.U. Sheleg, V.G. Hurtavy, A.V. Mudryi, M.Ya. Valakh, V.O. Yukhymchuk, I.S. Babichuk, M. Leon, R. Caballero, Study of structural and optical properties of $\text{Cu}_2\text{ZnSnS}_4$ semiconductor compounds thin films // *Semiconductors*, **48**(10), p. 1332-1338 (2014).
23. M. Grossberg, J. Krustok, J. Raudoja, T. Raadik, The role of structural properties on deep defect states in $\text{Cu}_2\text{ZnSnS}_4$ studied by photoluminescence spectroscopy // *Appl. Phys. Lett.* **101**, 102102–102106 (2012).